

Construction of monolayer $IrTe_2$ and the structural transition under low temperatures

Aiwei Wang(王爱伟), Ziyuan Liu(刘子媛), Jinbo Pan(潘金波), Qiaochu Li(李乔楚), Geng Li(李更), Qing Huan(郇庆), Shixuan Du(杜世萱), Hong-Jun Gao(高鸿钧)

Citation: Chin. Phys. B . 2020, 29(7): 078102 . **doi:** 10.1088/1674-1056/ab90eb
Journal homepage: http://cpb.iphy.ac.cn; http://iopscience.iop.org/cpb

What follows is a list of articles you may be interested in

Prediction of structured void-containing 1T-$PtTe_2$ monolayer with potential catalytic activity for hydrogen evolution reaction

Bao Lei(雷宝), Yu-Yang Zhang(张余洋), Shi-Xuan Du(杜世萱)

Chin. Phys. B . 2020, 29(5): 058104 . **doi:** 10.1088/1674-1056/ab8203

Magnetoelectric effect in multiferroic $NdMn_2O_5$

Syed Hamad Bukhari, Javed Ahmad

Chin. Phys. B . 2017, 26(1): 018103 . **doi:** 10.1088/1674-1056/26/1/018103

Phase transition of solid bismuth under high pressure

Hai-Yan Chen(陈海燕), Shi-Kai Xiang(向士凯), Xiao-Zhen Yan(颜小珍), Li-Rong Zheng(郑黎荣), Yi Zhang(张毅), Sheng-Gang Liu(刘盛刚), Yan Bi(毕延)

Chin. Phys. B . 2016, 25(10): 108103 . **doi:** 10.1088/1674-1056/25/10/108103

Bound states of Dirac fermions in monolayer gapped graphene in the presence of local perturbations

Mohsen Yarmohammadi, Malek Zareyan

Chin. Phys. B . 2016, 25(6): 068105 . **doi:** 10.1088/1674-1056/25/6/068105

InAs/GaAs submonolayer quantum-dot superluminescent diodes with active multimode interferometer configuration

Li Xin-Kun, Jin Peng, Liang De-Chun, Wu Ju, Wang Zhan-Guo

Chin. Phys. B . 2013, 22(4): 048102 . **doi:** 10.1088/1674-1056/22/4/048102

RAPID COMMUNICATION

Construction of monolayer $IrTe_2$ and the structural transition under low temperatures*

Aiwei Wang(王爱伟)[1,2,†], Ziyuan Liu(刘子媛)[1,2,†], Jinbo Pan(潘金波)[1,2], Qiaochu Li(李乔楚)[1,2], Geng Li(李更)[1,2,3,‡], Qing Huan(郇庆)[1], Shixuan Du(杜世萱)[1,2,3,4], and Hong-Jun Gao(高鸿钧)[1,2,3,4]

[1] *Beijing National Laboratory for Condensed Matter Physics and Institute of Physics, Chinese Academy of Sciences, Beijing* 100190, *China*
[2] *School of Physical Sciences, University of Chinese Academy of Sciences, Beijing* 100190, *China*
[3] *CAS Center for Excellence in Topological Quantum Computation, University of Chinese Academy of Sciences, Beijing* 100190, *China*
[4] *Songshan Lake Materials Laboratory, Dongguan* 523808, *China*

(Received 8 April 2020; revised manuscript received 19 April 2020; accepted manuscript online 7 May 2020)

Bulk iridium ditelluride ($IrTe_2$) is a layered material and is known for its interesting electronic and structural properties, such as large spin–orbit coupling, charge ordering, and superconductivity. However, so far there is no experimental study about the fabrication of monolayer $IrTe_2$. Here we report the formation of $IrTe_2$ monolayer on Ir(111) substrate by direct tellurization method. Scanning tunneling microscope (STM) images show the coexistence of 1/5 phase and 1/6 phase structures of $IrTe_2$ at room temperature. We also obtained STM images showing distorted stripe feature under low temperatures. This stripe feature is possibly induced by the strain between the $IrTe_2$ monolayer and the metal substrate. Density functional theory (DFT) calculations show that the $IrTe_2$ monolayer has strong interaction with the underlying Ir(111) substrate.

Keywords: $IrTe_2$, monolayer, phase transition, density functional theory

PACS: 81.05.zx, 81.07.-b **DOI:** 10.1088/1674-1056/ab90eb

1. Introduction

Two-dimensional (2D) materials have been widely investigated since the mechanical exfoliation of graphene in 2004.[1–5] Since then, many kinds of 2D materials have been studied, including graphene family (i.e., silicene,[6,7] germanene,[8] and stanene[9]), transition-metal dichalcogenides (TMDs),[10,11] and others.[12] Among them, Te-based 2D materials have attracted a lot of attention. For example, monolayer tungsten ditelluride (WTe_2) is a topologically nontrivial insulator and can be tuned to a superconductor by electric field.[13] Monolayer $MoTe_2$ has the property of structural phase transition.[14] Recently, $IrTe_2$ is widely studied because of its interesting electronic properties.[15–18] $IrTe_2$ has large spin–orbital coupling (SOC) which is considered as an origin of new physics such as topological phases.[17,19–21] Quasi-one-dimensional charge density wave (CDW) like stripe phase states are observed below 280 K with a wave vector $\boldsymbol{q} = (1/5, 0, -1/5)$ (i.e., 1/5 phase).[15,16,22] A superconducting gap is also observed below 3 K.[23] Although the bulk $IrTe_2$ crystal has been extensively investigated experimentally, the study of monolayer $IrTe_2$ has not been reported.

In this work, we report fabrication of monolayer $IrTe_2$ by direct tellurization of Ir(111) substrate. We find the coexistence of 1/5 and 1/6 stripe phases of the $IrTe_2$ film at room temperature (RT) using scanning tunneling microscope (STM). However, in bulk $IrTe_2$, the 1/5 phase can only be observed below 280 K,[15,16,22] and the 1/6 phase has been reported to exist below 85 K.[15] After cooling down the sample temperature to 190 K and 80 K, the 1/6 phase structure can still be seen, but the shape of the stripes tends to distort. The disordered stripes are found to cover the whole Ir(111) surfaces. Density functional theory (DFT) calculations show that $IrTe_2$ monolayer is metallic and it hybridizes strongly with the underlying Ir(111) substrate.

2. Methods

All the experiments are conducted in a home-built ultrahigh vacuum variable temperature STM system, equipped with flowing fluid-cooling head, as described elsewhere.[24] The base pressure of the chamber is 3×10^{-10} mbar. The single crystal Ir(111) surface is cleaned by repeated cycles of Ar^+ ion sputtering and annealing at 1470 K, till clean Ir(111) surface is verified by STM image and low electron energy diffraction (LEED) pattern. Tellurium (Te) (99.999%, Sigma-Aldrich company) is evaporated onto Ir(111) directly by a Knudsen cell (K-cell) evaporator at 480 K for 5 min. The substrate is

*Project supported by the National Key Research & Development Project of China (Grant Nos. 2019YFA0308500, 2018YFA0305800, and 2016YFA0202300), the National Natural Science Foundation of China (Grant Nos. 51991340, 61888102, and 11888101), and the Chinese Academy of Sciences (Grant Nos. XDB28000000 and XDB30000000).

†These authors contributed equally to this work.
‡Corresponding author. E-mail: gengli.iop@iphy.ac.cn

© 2020 Chinese Physical Society and IOP Publishing Ltd

kept at 780 K during evaporating. The deposition rate of Te is calibrated by depositing Te onto Ag(111) substrate. The STM characterization is conducted at room temperature (RT), 190 K, and 80 K, respectively, in a constant-current mode with a bias voltage added to the sample.

In density functional theory calculations, the geometric relaxations are carried out using the VASP code[25,26] with projector-augmented wave (PAW) potentials[27,28] and Perdew–Burke–Ernzerhof (PBE) parametrization of generalized gradient approximation (GGA).[29] A plane-wave basis set with an energy cutoff of 400 eV is used. The periodic slab model includes four layers of Ir, one layer of $IrTe_2$, and a vacuum layer of 20 Å. A $5\times5\times1$ Γ-point centered k-point mesh is applied to sample the Brillouin zone. All atoms are fully relaxed, except for the bottom two substrate layers. The structures are fully relaxed until the energy and force are converged to 10^{-5} eV and 0.01 eV/Å, respectively.

3. Results and discussion

Figure 1 shows schematically the process of growing $IrTe_2$ on Ir(111) substrate. First, we directly deposit tellurium on Ir(111) substrate as shown in the left panel of Fig. 1. Then we anneal the sample at 780 K for 10 min to ensure the tellurization of the substrate. Finally, the $IrTe_2$ layer is fabricated.

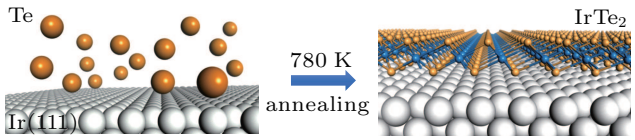


Fig. 1. Schematic showing the formation of $IrTe_2$ monolayer on Ir(111) substrate by direct tellurization method.

Figure 2(a) shows an STM image of $IrTe_2$ monolayer acquired at RT. Figure 2(b) is a higher-resolution image of the same region. The lattice constant is measured to be about 0.42 ± 0.02 nm, similar to that of the bulk $IrTe_2$, 0.39 nm.[16] The difference is probably caused by the interaction between the $IrTe_2$ monolayer and the underlying Ir(111) substrate, which will be discussed later. The stripe feature is clearly seen in Figs. 2(a) and 2(b), and is highlighted with green rectangles in Fig. 2(b) to guide the eyes. The stripes are attributed to the 1/5 phase of $IrTe_2$ which emerges as a first-order phase transition from the (1×1) phase under low temperature.[15,22,30,31] The 1/5 phase is resulted from the dimerization of Ir–Ir.[15,31] When the two dimerized segments of Ir atoms are separated by three undimerized rows of Ir atoms, the 1/5 phase is formed.[15,31] However, in bulk $IrTe_2$ crystal, the transition temperature is about 280 K.[15,16,22] The observation of the 1/5 phase at RT suggests an increasing of the transition temperature for the $IrTe_2$ monolayer on Ir(111) surface. The decreasing of the layer thickness leads to a significant change of the phase transition temperature.

Interestingly, on the same sample, another feature is also observed at RT, as shown in Fig. 2(c). Herringbone feature can be resolved from the image and the small black spots are attributed to the Te atomic vacancies. A higher-resolution STM image is shown in Fig. 2(d). The periodicity of the herringbone feature is about 2.2 nm. We note that some regions in Figs. 2(a) and 2(c) look fuzzy and they are likely due to the fast moving atoms on the $IrTe_2$ surface at RT, which cannot be well captured by STM due to the slow scanning.[32–34] This herringbone structure reminds us of the 1/6 phase of $IrTe_2$.[15,31,35] The 1/6 phase is caused by the alternating of two adjacent dimerized segments of Ir atoms, while the segments are separated by an undimerized row of Ir atoms, and rotated 120° with respect to each other.[15,31,35] However, in bulk $IrTe_2$, the 1/6 phase can only be achieved below 85 K, since it is the ground state of $IrTe_2$.[15,31] Se-doped $IrTe_2$ was reported to have the 1/6 phase charge order at RT due to Ir–Ir dimerization, which is caused by Se doping induced strain.[17,18,35] The reason that the 1/6 phase is observed in monolayer $IrTe_2$ at RT is currently not clear.

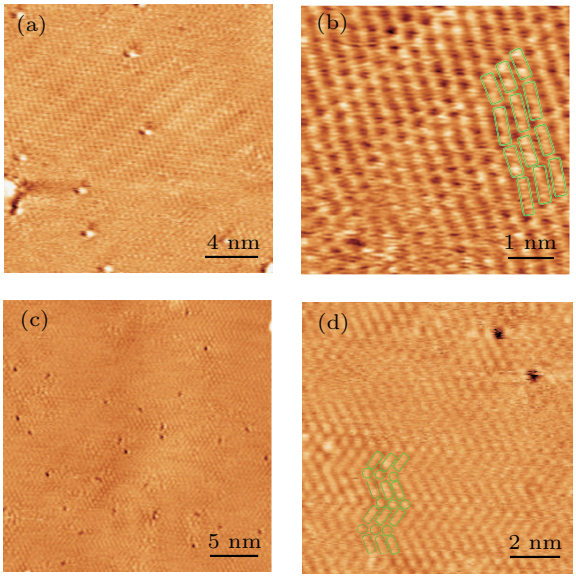


Fig. 2. STM images of $IrTe_2$ monolayers taken at RT. (a) Scanning parameters $V_s=0.06$ V, $I_t=0.1$ nA. (b) Higher-resolution image showing the 1/5 phase stripe features, as marked by the green rectangles. Scanning parameters $V_s=0.1$ V, $I_t=0.1$ nA. (c) STM image of $IrTe_2$ monolayer taken at another area on the same sample. Scanning parameters $V_s=-0.11$ V, $I_t=0.1$ nA. (d) Higher-resolution image showing the herringbone-like 1/6 phase stripe features, as marked by the green rectangles and circles. Scanning parameters $V_s=0.11$ V, $I_t=0.1$ nA.

In order to explore the possible phase transition of monolayer $IrTe_2$ at low temperature, we performed temperature dependent STM studies. Figures 3(a) and 3(b) show large-size and small scale STM images obtained at 190 K. While the herringbone feature of the 1/6 phase can still be resolved, the stripes tend to bend and form a disordered structure on the surface. The disordered structure covers the whole sample surface and is never seen at RT. At 80 K, the disordered feature becomes more significant, as shown in Figs. 3(c) and 3(d).

The lower the temperature, the more distorted the stripes. The corrugation of the disordered feature is much smaller than the height of a typical atomic step (∼ 2 Å), as shown in the inset of Fig. 3(d). The formation of this kind of disordered feature may be related to the competition between the ordering of the $IrTe_2$ monolayer and the strain of the underlying Ir(111) substrate.[9] Since the stripe features of $IrTe_2$ are caused by the Ir–Ir dimerization,[15,31] the disordered stripes are possibly due to the random Ir–Ir dimerization induced by the strain in the $IrTe_2$ film. If that is the case, our observation suggests a strong interaction between the $IrTe_2$ layer and the Ir substrate.

In order to investigate the interaction and electronic properties of $IrTe_2$ on Ir(111) surface, we calculate the electronic structures based on a supercell with 2×2 $IrTe_2$ on 3×3 Ir(111) lattice (Fig. 4(a)). The Ir atoms in $IrTe_2$ and Ir(111) substrate are represented by green and silver balls, respectively, and the Te atoms are represented by brown balls. Because the STM images show complex structures of the $IrTe_2$ layer, we use a small supercell with less lattice mismatch to do the calculations. The calculated projected band structure on $IrTe_2$ is presented in Fig. 4(b). The sizes of blue circles correspond to the contribution of the $IrTe_2$ monolayer. The band structure indicates that the $IrTe_2$ on Ir(111) surface is metallic and strongly hybridized with the underlying Ir(111) substrate. Indeed, differential charge density shows the apparent charge accumulation at the interface, indicating the strong interaction between the $IrTe_2$ layer and substrate, as shown in Figs. 4(c) and 4(d). This gives a possible explanation to the driving force of the formation of the distorted stripes that we observe under low temperature.

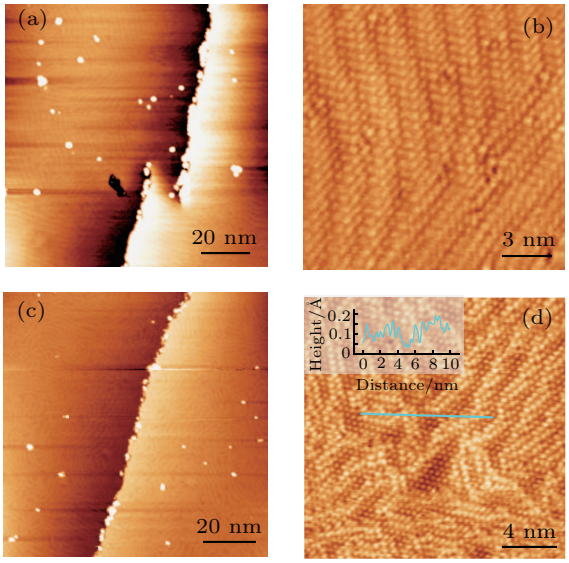


Fig. 3. STM images of $IrTe_2$ monolayers taken at 190 K and 80 K, respectively. (a) STM image of $IrTe_2$ monolayer taken at 190 K, showing the large-scale disordered feature of the stripes. Scanning parameters $V_s = -0.5$ V, $I_t = 0.1$ nA. (b) Higher-resolution image showing the disordered 1/6 phase structure. Scanning parameters $V_s = -0.3$ V, $I_t = 0.1$ nA. (c) STM image of $IrTe_2$ monolayer taken at 80 K. Scanning parameters $V_s = -0.5$ V, $I_t = 0.1$ nA. (d) Higher-resolution image of $IrTe_2$ monolayer at 80 K. Line profile shows the corrugation of the surface is ∼ 0.2 Å. Scanning parameters $V_s = -0.2$ V, $I_t = 0.1$ nA.

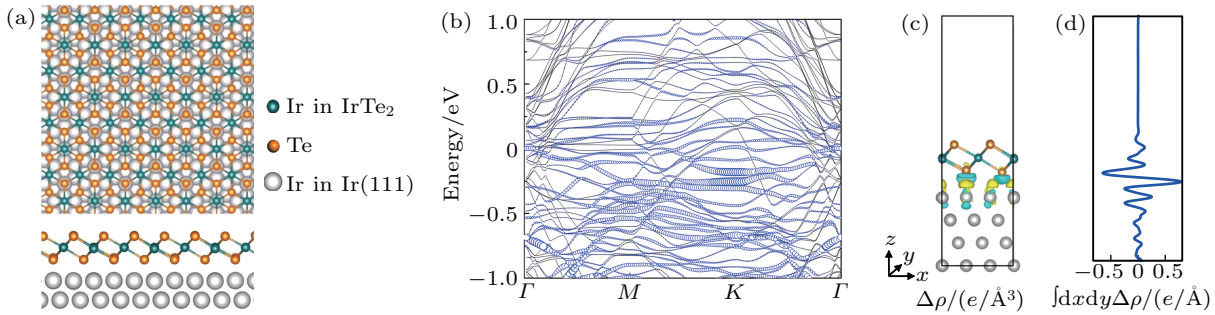


Fig. 4. DFT results of $IrTe_2$ monolayer on Ir(111) substrate. (a) Top and side views of the optimized model, showing 2×2 $IrTe_2$ on a 3×3 Ir(111) lattice. (b) Calculated band structure of the structure in (a). (c) Differential charge density for $IrTe_2$/Ir(111). Here, $\Delta\rho = \rho[IrTe_2/Ir(111)] - \rho[IrTe_2] - \rho[Ir(111)]$, and yellow corresponds to electron accumulation, while green corresponds to electron loss. The isosurface value is 0.034 $e/Å^3$. Obvious charge transfer occurs, resulting in a strong interaction between the $IrTe_2$ monolayer and Ir(111) surfaces. (d) Integrated electron density difference for $IrTe_2$/Ir(111). Negative value means electron loss, while positive value means electron accumulation.

4. Conclusion

We report the growth of the $IrTe_2$ monolayer on Ir(111) substrate. At room temperature, we observed the 1/5 phase and 1/6 phase of $IrTe_2$, suggesting that the reduction of the layer thickness has significantly increased the transition temperatures. We also obtained disordered stripe features at low temperatures, which is possibly induced by the strain between the $IrTe_2$ monolayer and the metal substrate. DFT calculations show that the monolayer $IrTe_2$ on Ir substrate is metallic and the interaction between $IrTe_2$ and Ir substrate is strong.

References

[1] Novoselov K S, Geim A K, Morozov S V, Jiang D, Zhang Y, Dubonos S V, Grigorieva I V and Firsov A A 2004 *Science* **306** 666
[2] Zhang G Y, Du S X, Wu K H and Gao H J 2018 *Science* **360** 673
[3] Pan Y, Zhang L Z, Huang L, Li L F, Meng L, Gao M, Huan Q, Lin X, Wang Y L, Du S X, Freund H J and Gao H J 2014 *Small* **10** 2215
[4] Liu Y, Weiss N O, Duan X D, Cheng H C, Huang Y and Duan X F 2016 *Nat. Rev. Mater.* **1** 16042
[5] Duong D L, Yun S J and Lee Y H 2017 *ACS Nano* **11** 11803
[6] Meng L, Wang Y L, Zhang L Z, Du S X, Wu R T, Li L F, Zhang Y, Li G, Zhou H T, Hofer W A and Gao H J 2013 *Nano Lett.* **13** 685
[7] Li G, Zhang L Z, Xu W Y, Pan J B, Song S R, Zhang Y, Zhou H T, Wang Y L, Bao L H, Zhang Y Y, Du S X, Ouyang M, Pantelides S T and Gao H J 2018 *Adv. Mater.* **30** 1804650

[8] Li L F, Lu S Z, Pan J B, Qin Z H, Wang Y Q, Wang Y L, Cao G Y, Du S X and Gao H J 2014 *Adv. Mater.* **26** 4820

[9] Zhu F F, Chen W J, Xu Y, Gao C L, Guan D D, Liu C H, Qian D, Zhang S C and Jia J F 2015 *Nat. Mater.* **14** 1020

[10] Wang Q H, Kalantar-Zadeh K, Kis A, Coleman J N and Strano M S 2012 *Nat. Nanotechnol.* **7** 699

[11] Chhowalla M, Shin H S, Eda G, Li L J, Loh K P and Zhang H 2013 *Nat. Chem.* **5** 263

[12] Tan C L, Cao X H, Wu X J, He Q Y, Yang J, Zhang X, Chen J Z, Zhao W, Han S K, Nam G H, Sindoro M and Zhang H 2017 *Chem. Rev.* **117** 6225

[13] Fatemi V, Wu S F, Cao Y, Bretheau L, Gibson Q D, Watanabe K J, Taniguchi T, Cava R J and Jarillo-Herrero P 2018 *Science* **362** 926

[14] Wang Y, Xiao J, Zhu H Y, Li Y, Alsaid Y, Fong K Y, Zhou Y, Wang S Q, Shi W, Wang Y, Zettl A, Reed E J and Zhang X 2017 *Nature* **550** 487

[15] Chen C, Kim J S, Yang Y F, Cao G X, Jin R Y and Plummer E W 2017 *Phys. Rev. B* **95** 094118

[16] Ko K T, Lee H H, Kim D H, Yang J J, Cheong S W, Eom M J, Kim J S, Gammag R, Kim K S, Kim H S, Kim T H, Yeom H W, Koo T Y, Kim H D and Park J H 2015 *Nat. Commun.* **6** 7342

[17] Pascut G L, Birol T, Gutmann M J, Yang J J, Cheong S W, Haule K and Kiryukhin V 2014 *Phys. Rev. B* **90** 195122

[18] Oh Y S, Yang J J, Horibe Y and Cheong S W 2013 *Phys. Rev. Lett.* **110** 127209

[19] Bernevig B A, Hughes T L and Zhang S C 2006 *Science* **314** 1757

[20] Hasan M Z and Kane C L 2010 *Rev. Mod. Phys.* **82** 3045

[21] Yang J J, Choi Y J, Oh Y S, Hogan A, Horibe Y, Kim K, Min B I and Cheong S W 2012 *Phys. Rev. Lett.* **108** 116402

[22] Pascut G L, Haule K, Gutmann M J, Barnett S A, Bombardi A, Artyukhin S, Birol T, Vanderbilt D, Yang J J, Cheong S W and Kiryukhin V 2014 *Phys. Rev. Lett.* **112** 086402

[23] Kim H S, Kim S R, Kim K, Min B I, Cho Y H, Wang L H, Cheong S W and Yeom H W 2016 *Nano Lett.* **16** 4260

[24] Wu R T, Yan L H, Zhang Y F, Ren J H, Bao D L, Zhang H G, Wang Y L, Du S X, Huan Q and Gao H J 2015 *J. Phys. Chem. C* **119** 8208

[25] Kresse G 1996 *Phys. Rev. B* **54** 11169

[26] Kresse G and Furthmiiller J 1996 *Comput. Mater. Sci.* **6** 15

[27] Blochl P E 1994 *Phys. Rev. B* **50** 17953

[28] Kresse G 1999 *Phys. Rev. B* **59** 1758

[29] Perdew J P, Burke K and Ernzerhof M 1996 *Phys. Rev. Lett.* **77** 3865

[30] Machida T, Fujisawa Y, Igarashi K, Kaneko A, Ooi S, Mochiku T, Tachiki M, Komori K, Hirata K and Sakata H 2013 *Phys. Rev. B* **88** 245125

[31] Hsu P J, Mauerer T, Vogt M, Yang J J, Oh Y S, Cheong S W, Bode M and Wu W D 2013 *Phys. Rev. Lett.* **111** 266401

[32] Huang T, Zhao J, Peng M, Popov A A, Yang S F, Dunsch L and Petek H 2011 *Nano Lett.* **11** 5327

[33] Lu H L, Cao Y, Qi J, Bakker A, Strassert C A, Lin X, Ernst K H, Du S X, Fuchs H and Gao H J 2018 *Nano Lett.* **18** 4704

[34] Harikumar K R, Polanyi J C, Sloan P A, Ayissi S and Hofer W A 2006 *J. Am. Chem. Soc.* **128** 16791

[35] Dai J X, Haule K, Yang J J, Oh Y S, Cheong S W and Wu W D 2014 *Phys. Rev. B* **90** 235121